Pergamon

0277-5387(94)00305-X

Polyhedron Vol. 14, No. 6, pp. 771–780, 1995

0277-5387/95 $9.50+0.00

ELECTROCHEMICAL STUDIES OF IRON(III) SCHIFF BASE COMPLEXES—II. DIMERIC μ-OXO[$Fe^{III}(N_2O_2)$]$_2$O COMPLEXES

J.-P. COSTES and J.-B. TOMMASINO

Laboratoire de Chimie de Coordination du CNRS, UP 8241, lié par conventions à l'Université Paul Sabatier et à l'Institut National Polytechnique de Toulouse, 205, route de Narbonne, 31077 Toulouse Cedex, France

and

B. CARRÉ

Laboratoire de Synthèse et d'Etudes Physicochimiques Organiques, Faculté des Sciences, Parc de Gramont, 37200 Tours, France

and

F. SOULET and P.-L. FABRE*

Laboratoire de Chimie Inorganique, EA 807, Université Paul Sabatier, 118, route de Narbonne, 31062 Toulouse Cedex, France

(*Received* 16 *February* 1994; *accepted* 27 *July* 1994)

Abstract—The electrochemical reduction of μ-oxo bridged Fe^{III} dimers (L)Fe—O—Fe(L), where L is a Schiff base, has been investigated in aprotic solvents by cyclic voltammetry and coulometry with UV–vis spectroscopy. Three complexes deriving from Schiff base ligands with N_2O_2 environments are described. The reduction of (L)Fe^{III}—O—Fe^{III}(L) occurs at a potential around -1 V/SCE and releases the monomeric Fe^{II}(L) complex. A mechanism is proposed using high speed cyclic voltammetry. The reduction pattern is affected by dioxygen through the high reactivity of Fe^{II}(L). These μ-oxo bridged Fe^{III} dimers (L)Fe—O—Fe(L) can also be cleaved by Cl^- addition and yield the monomeric Fe^{III}(L) complexes. Finally, the Fe—O bond is not so strong because it cleaves either by electrochemical reduction or by chemical addition of Cl^-.

In the chemistry of dioxygen activation, iron is one of the most involved metals.[1,2] In this context, the μ-oxo-bridged dinuclear complexes Fe—O—Fe have been studied extensively with respect to their structural, magnetic and spectroscopic properties and are potentially models of biological systems.[2,3]

In recent years, synthetic efforts have been made in modelling the diferrous active sites of the oxo-proteins.[4–6] In these proteins, the active centre exists under the various oxidation states: a reduced Fe^{II}_2, a mixed valence $Fe^{II}Fe^{III}$ and an oxidized Fe^{III}_2 form. Among the various models,[3] the best models eem to be those which contain the μ-oxo-bis(μ-carboxylate) bridges[6] or at least a μ-carboxylate bridge.[4] In this way the chemistry of iron Schiff base complexes has been investigated.[7,8] The Fe_2(salmp)$_2$ complex exhibits the smallest Fe—O—Fe angle and Fe—Fe separation.[8] Moreover, the three oxidation levels are related by reversible redox reaction.

In connection with our work on iron Schiff bases,[9] we have followed the reactivity of mono-

* Author to whom correspondence should be addressed.

meric $Fe^{III}(L)Cl$ towards dioxygen. Under reduction, the Fe^{II} complex is extremely reactive[10] and yields upon oxygenation the simplest μ-oxo-bridged[3] dinuclear complexes $(L)Fe^{III}$—O—$Fe^{III}(L)$. These compounds exhibit strong antiferromagnetic coupling between the two high spin Fe^{III} ions, which is dependent on the Fe—O—Fe bond angle.[7] Unfortunately, these complexes present no reactivity towards dioxygen and seem to be thermodynamic wells. The electrochemical reduction of $[Fe(SALEN)]_2O$ was first reported by Schultz *et al.*[11] but the mechanism is not clear. In this paper (Part II), we describe the electrochemical behaviour of three complexes $(L)Fe^{III}$—O—$Fe^{III}(L)$, where L is an N_2O_2 Schiff base (SALEN type, see part I[9]): H_2AEAP = *N,N'*-ethylene (acetylacetoneimine) (hydroxyacetophenoneimine);[12] H_2SALEN = *N,N'*-ethylene-bis(salicylideneimine);[13] $H_2SALOPH$ = *N,N'*-orthophenylene-bis(salicylideneimine).[13] The complexes are referred to as $[Fe(AEAP)]_2O$, $[Fe(SALEN)]_2O$[14] and $[Fe(SALOPH)]_2O$.[15]

EXPERIMENTAL

Products

The Schiff bases were prepared according to literature methods through the well-known amine–aldehyde (or ketone) condensation: H_2AEAP,[12] H_2SALEN[13] and $H_2SALOPH$.[13] The monomeric complexes $Fe^{III}(L)Cl$ were synthesized by complexation of $FeCl_3$ with the protonated ligand H_2L in basic methanol: Fe(AEAP)Cl,[16] Fe(SALEN)Cl[13] and Fe(SALOPH)Cl.[13] They are used for the synthesis of the μ-oxo$(L)Fe^{III}$—O—$Fe^{III}(L)$ complexes through an acid–base reaction: $[Fe(SALEN)]_2O$[14] and $[Fe(SALOPH)]_2O$.[15]

$[Fe(AEAP)]_2O$

To a suspension of 0.5 g of Fe(AEAP)Cl in 20 cm^3 aqueous solution was added 0.5 cm^3 of triethylamine, NEt_3. Within 15 min, an orange solid precipitated, which was filtered and dried (0.45 g, 98%). The compound was recrystallized in methanol–isopropyl alcohol and dried *in vacuo*. Found: C, 55.1; H, 5.5; N, 8.4. Calc. for $C_{30}H_{32}Fe_2N_4O_5$: C, 55.9; H, 5.6; N, 8.7%.

Physical measurements

Electrochemical measurements were carried out with home-made potentiostats controlled by an Apple IIe microcomputer[17] or by a PC for high speed cyclic voltammetry (from 10 to 2000 V s^{-1}).[18] The electrochemical cell was a conventional one with three electrodes [working electrode: platinum (diameter 2 mm, EDI, Tacussel) for analytical purposes, platinum microelectrode (diameter 100 μm) for kinetics analysis and platinum foil for electrolysis; counter electrode: platinum wire; reference electrode: Ag/AgCl, KCl 0.1 mol dm^{-3} or SCE]; the potentials are given vs the SCE in the tables. The supporting electrolyte Bu_4NPF_6 (Aldrich, electroanalytical grade) was used as received. Acetonitrile, CH_3CN (Aldrich, Gold Label), was used without any further purification while dichloromethane, CH_2Cl_2 (SDS, Purex), was passed over alumina prior to use. UV–vis spectroscopic measurements were conducted with an UVIKON 930 spectrophotometer (Kontron Instruments).

RESULTS AND DISCUSSION

Within the electroactivity domain of the solvent, the general voltammogram shows two distinct electrode processes (Fig. 1):

(1) An oxidation process around 1 V which is attributed to the Schiff base oxidation. This oxidation leads to the polymerization of the complexes on the electrode surface and is a way to obtain modified electrodes.[19,20] By high speed voltammetry, it has been shown that the oxidation is reversible so that their formal oxidation potential can be obtained. Moreover, the polymerization may go through a radical cation–radical cation coupling of the phenyl group.[20]

(2) A reduction process around −1.1 V which appears more or less reversible according to the nature of the base and the potential scan speed. This process corresponds to the reduction of the μ-oxo complex. As with $[Fe(SALEN)]_2O$ in DMSO[10] or in DMF,[21] these reductions seem to proceed through a one-electron exchange by comparison with the well known ferrocene electrochemical

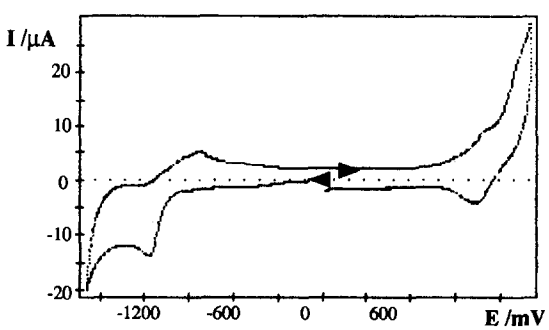

Fig. 1. General voltammogram of $[Fe(L)]_2O$ complexes at a platinum electrode in CH_2Cl_2–Bu_4NPF_6 (0.1 mol dm^{-3}), potential sweep rate 0.1 V s^{-1}: $[Fe(SALEN)]_2O$, 1 mmol dm^{-3}.

system. In any case, whatever the solvent, CH_3CN or CH_2Cl_2, we do not observe a second reduction of the complexes as in DMSO.[10] This second reduction process, which is near the solvent discharge, has been attributed to the reduction into the Fe^{II}_2 form, but may be interpreted by the ligand reduction, as for Ni(SALOPH), which yields dimeric species.[22]

In the sequel, the study is restricted to the electrochemical reduction in the μ-oxo complexes, which appears around -1.1 V (Fig. 1). Earlier electrochemical studies of $[Fe(SALEN)]_2O$ in DMSO[10] have shown that the reduction process is more complicated than a single electron transfer which affords the mixed valence Fe^{III} Fe^{II} complexes. The apparent electron number varies and is greater than 1.

As for the monomeric Fe(L)Cl complexes,[9] the voltammograms of the different complexes present the same shape (Fig. 2). As expected, the reduction potential of $[Fe(L)]_2O$ depends on the nature of the Schiff base. The increase in the electronic delocalization of the Schiff base ring (with the number of aromatic rings) shifts the redox potential towards the anodic side: it makes the electrochemical reduction of Fe^{III} into Fe^{II} easier.

Under stationary conditions (Table 1) at a rotating platinum disc electrode, the voltammograms show the diffusion-controlled wave of the reduction of the complexes. Exhaustive electrolysis of $[Fe(L)]_2O$ at the potential -1.3 to -1.5 V show that there is a bielectronic exchange. With L = SALEN, the orange solution ($\lambda = 450$ nm) turns light yellow ($\lambda = 280$ nm). Electrolysis has to be carried out under drastic anaerobic conditions in order to avoid reoxidation of the products by dioxygen and to obtain an electron exchange higher than 2. Then, the electrochemical reduction of these complexes should yield Fe^{II}_2 species. This bielectronic exchange matches the diffusion currents measured under stationary conditions. In CH_3CN or CH_2Cl_2, the limiting currents obey the Levich law; they are proportional to the square root of the electrode rotation speed (Fig. 3), as for a diffusion-controlled process. According to the Levich law, we obtained in CH_2Cl_2 an average diffusion coefficient of 3.5×10^{-6} cm^2 s^{-1}. In CH_3CN, we observed some passivation phenomena, especially when L is SALOPH. This passivation may be attributed to the low solubility of $[Fe(SALOPH)]_2O$ or to the imine bond reduction of the base (L),[23] yielding a C—C bond and then polymeric deposits. This implies direct reduction of the base or electron transfer from the metal to the base.[24]

Table 1. Electrochemical characteristics under stationary conditions of $[Fe^{III}(L)]_2O$ complexes (1 mmol dm^{-3}: Pt rotating electrode, 1000 t min^{-1})

	$E_{1/2}$ (mV)	I_D (μA)	p (mV)
Solvent CH_2Cl_2, Bu_4NPF_6, 0.1 mol dm^{-3}			
$[Fe(AEAP)]_2O$	-1508	-20.3	114
$[Fe(SALEN)]_2O$	-1158	-25	102
$[Fe(SALOPH)]_2O$[a]	-1007	-8.5	96
Solvent, CH_3CN, Bu_4NPF_6, 0.1 mol dm^{-3}			
$[Fe(AEAP)]_2O$	-1290	-7.9	140
$[Fe(SALEN)]_2O$	-1098	-36.9	75
$[Fe(SALOPH)]_2O$[b]	-969	-2.4	121

[a] For 0.5 mmol dm^{-3}.

[b] Sparingly soluble, <0.5 mmol dm^{-3}.

p = slope of the linear regression of $E = f$ (log $|I_D - I/I|$).

Cyclic voltammetry at millimetric electrodes

At a platinum electrode, the voltammograms depend on the nature of the Schiff base as men-

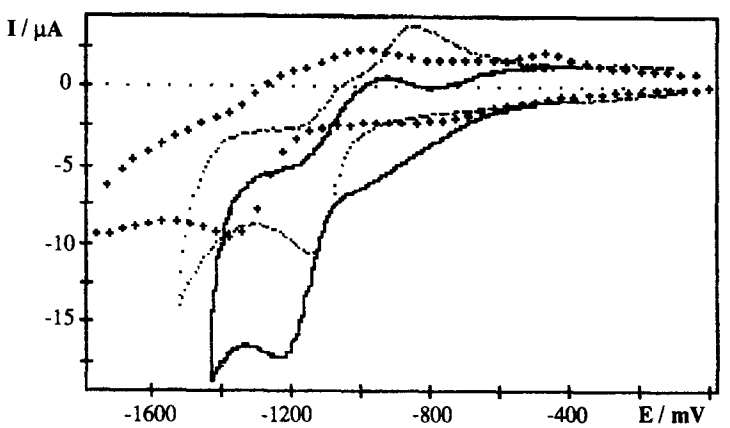

Fig. 2. Cyclic voltammograms at a platinum electrode in CH_2Cl_2–Bu_4NPF_6 (0.1 mol dm^{-3}) of $[Fe(L)]_2O$, potential sweep rate 0.1 V s^{-1}. L = AEAP (+ + +) 1 mmol dm^{-3}, SALEN (——) 2 mmol dm^{-3}, SALOPH (···) 1 mmol dm^{-3}.

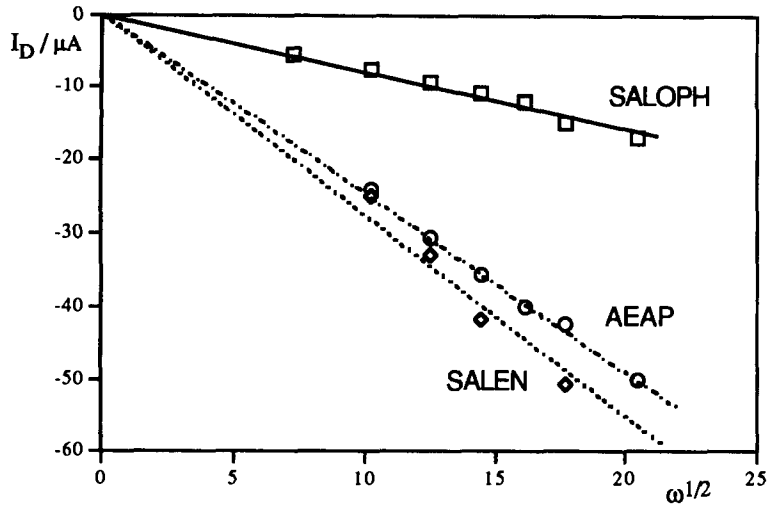

Fig. 3. Limiting current I_D vs $\omega^{1/2}$ for $[Fe(L)]_2O$ in CH_2Cl_2–Bu_4NPF_6 (0.1 mol dm^{-3}); platinum electrode: L = AEAP 1 mmol dm^{-3}, SALEN 1 mmol dm^{-3}, SALOPH 0.5 mmol dm^{-3}.

tioned above (Fig. 2), but they present the same shape. Beside the thermodynamic influence of the Schiff base, the delocalization on the base increases the kinetics of the electron transfer. By cyclic voltammetry (Table 2), the peak separation ΔE_p is decreased and the peak ratio RI_p increases: the reduced product is stabilized. Figure 4 shows the variation of the voltammograms as a function of the potential sweep rate v. At low speed v ($v = 0.02$ V s^{-1}), the electrochemical system does not appear reversible. When the sweep rate is increased, the reverse oxidation peak at ≈ -1.05 V appears and increases. Moreover, a secondary backward oxidation peak arises around -0.8 V. The electrochemical reduction of $[Fe(L)]_2O$ is more complicated than a simple electron transfer. The plots of the reduction peak I_p vs the square root of the potential scan rate $\sqrt{v}$ are not linear as for pure electron transfer.[26] At low speed, the current related to $\sqrt{v}$ matches with bielectronic transfer, while at high speed (in the domain of speed for millimetric electrodes[18]) it matches monoelectronic transfer. This means that in a first step the reduction yields the mixed valence $(L)Fe^{III}$—O—$Fe^{II}(L)$ form which is not stable. The appearance of the oxidation peak at ≈ -0.8 V can be attributed to the oxidation of $Fe^{III}(L)OH$.[10,21] These hydroxy species are not stable because acid–base titrations of Fe(SALEN)[27] or Fe(SALOPH)[28] always yield the μ-oxo-bridged dinuclear complexes $(L)Fe^{III}$—O—$Fe^{II}(L)$ in DMSO–H_2O, according to:

$$2Fe(L)^+ + H_2O \rightleftharpoons \mu\text{-O-}[Fe(L)]_2 + 2H^+ \quad (1)$$

$K_D = 5 \times 10^{-13}$ for L = SALEN or

1.5×10^{-12} for L = SALOPH,[27,28]

where the titration reaction is

Table 2. Electrochemical characteristics by cyclic voltammetry of $[Fe^{III}(L)]_2O$ complexes (1 mmol dm^{-3}, Pt electrode, potential scan speed 0.1 V s^{-1})

	$E_{p\,red}$ (mV)	ΔE_p (mV)	$I_{p\,red}$ (μA)	RI_p
Solvent CH_2Cl_2, Bu_4NPF_6, 0.1 mol dm^{-3}				
$[Fe(AEAP)]_2O$	−1382	183	−9.2	0.29
$[Fe(SALEN)]_2O$	−1195	127	−11.3	0.48
$[Fe(SALOPH)]_2O^a$	−1052	85	−5.1	0.59
Solvent CH_3CN, Bu_4NPF_6, 0.1 mol dm^{-3}				
$[Fe(AEAP)]_2O$	−1367	157	−6.9	0.32
$[Fe(SALEN)]_2O$	−1230	129	−10.6	0.64
$[Fe(SALOPH)]_2O^b$	−989	544	−1.1	0.69

[a] For 0.5 mmol dm^{-3}.

[b] Sparingly soluble, <0.5 mmol dm^{-3}.

$\Delta E_p = E_{p\,backward} - E_{p\,forward} = E_{p\,ox} - E_{p\,red}$ and $RI_p = |I_{p\,backward}/I_{p\,forward}|$.

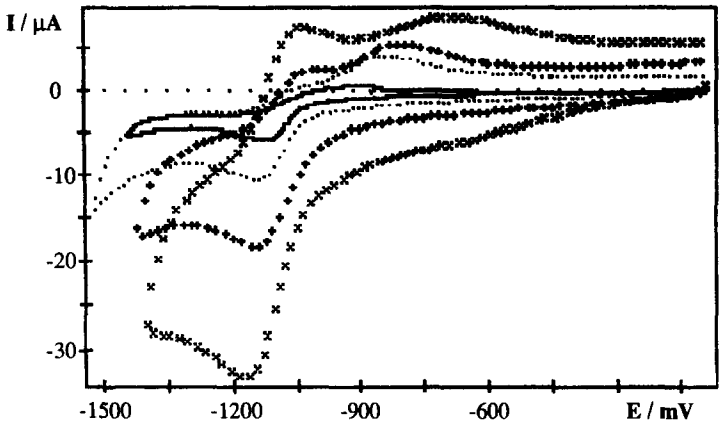

Fig. 4. Cyclic voltammograms at a platinum electrode in CH_2Cl_2–Bu_4NPF_6 (0.1 mol dm^{-3}) of $[Fe(SALEN)]_2O$, 1 mmol dm^{-3} for various potential sweep rate: v (V s^{-1}) = 0.02 (——), 0.1 (· · ·), 0.4 (+ + +) and 1 (× × ×).

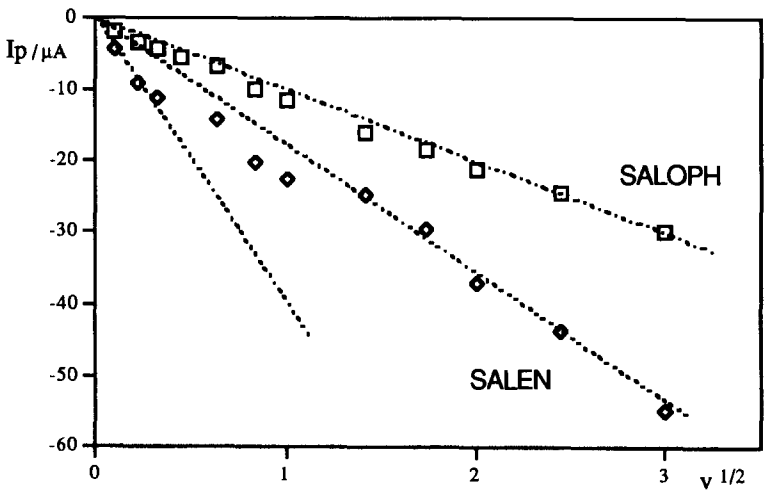

Fig. 5. Plots of $|I_{p\,red}|$ vs $\sqrt{v}$ (potential scan rate) for $[Fe(L)]_2O$ in CH_2Cl_2–Bu_4NPF_6 (0.1 mol dm^{-3}), platinum electrode (diam. 2 mm). L = SALEN, 1 mmol dm^{-3}; SALOPH, 0.5 mmol dm^{-3}.

$$2Fe(L)^+ + 2OH^- \rightleftharpoons \mu\text{-O-}[Fe(L)]_2 + H_2O. \quad (2)$$

These results imply cleavage of the Fe—O bond of the mixed valence $(L)Fe^{III}$—O—$Fe^{II}(L)$ form. The overall process may be expressed as follows:

$$(L)Fe^{III}\text{—O—}Fe^{III}(L) + e^- \rightleftharpoons [(L)Fe^{III}\text{—O—}Fe^{II}(L)]^- \quad E \quad (3)$$

$$[(L)Fe^{III}\text{—O—}Fe^{II}(L)]^- \rightarrow (L)Fe^{II} + (L)Fe^{III}\text{—}O^- \quad C \quad (4)$$

$$(L)Fe^{III}\text{—}O^- + H_2O \rightarrow (L)Fe^{III}\text{—OH} + OH^- \quad C \quad (5)$$

$$(L)Fe^{III}\text{—OH} + e^- \rightleftharpoons [(L)Fe^{II}\text{—OH}]^- \quad E. \quad (6)$$

The first electrochemical step (3) at ≈ -1.1 V yields the mixed valence form which is not stable. Reaction (4) is the Fe—O bond cleavage into $(L)Fe^{II}$ and $(L)Fe^{III}$—O^-, which may react with residual water according to reaction (5). At the potential where the reduction of $[Fe(L)]_2O$ is observed, the hydroxy compound is reduced because its potential is more anodic (≈ -0.8 V[10,21]). This reaction scheme explains the bielectronic exchange at low potential scan speed or under stationary conditions: the kinetics of the Fe—O bond cleavage drives the overall process. Moreover, electrolysis conducted in air-tight cells leads to the determination of two electrons per complex; the UV–vis spectra match the one of $Fe^{II}(L)$ yielded by electrolysis of $Fe^{III}(L)Cl$. The $Fe^{II}(L)$ complexes are extremely reactive towards dioxygen to yield the μ-oxo complexes, which are observed in Fig. 6 when dioxygen traces are present. With no dioxygen, the voltammogram shows the classical pattern of the $[Fe(L)]_2O$ reduction. It is a poorly reversible system that gives the formation of $[(L)Fe^{II}\text{—OH}]^-$, which is detected on the backward scan by a peak around

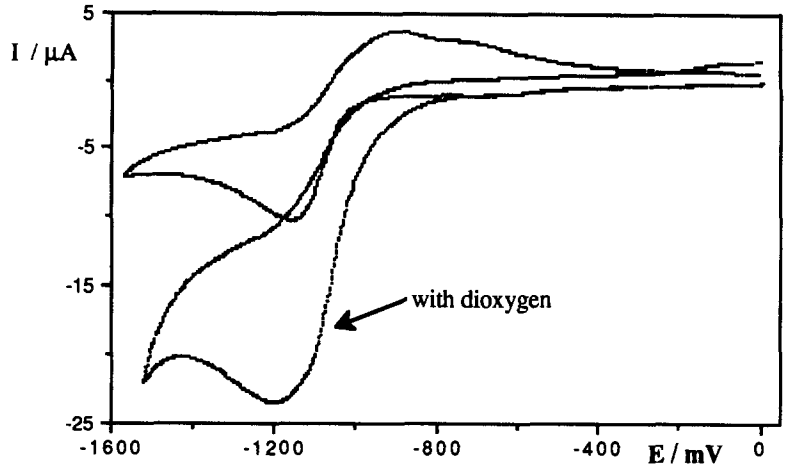

Fig. 6. Dioxygen action on the cyclic voltammograms at a platinum electrode in CH_2Cl_2–Bu_4NPF_6 (0.1 mol dm^{-3}) of $[Fe(SALOPH)]_2O$, 1 mmol dm^{-3} (v = 0.1 V s^{-1}).

−0.8 V. With dioxygen traces, the voltammogram is modified: no backward peaks are observed and the reduction peak current of $[Fe(L)]_2O$ is increased as for a catalytic process. The interaction with dioxygen goes through the monomeric $(L)Fe^{II}$, which reacts with dioxygen[9] according to:

$$2(L)Fe^{II} + 1/2O_2 \rightarrow [(L)Fe—O—Fe(L)]. \quad (7)$$

This confirms the high reactivity of the $Fe^{II}(L)$ species and the cleavage of the Fe—O bond. However, according to the proposed scheme, $Fe^{II}(L)$ is produced and should be detected by an oxidation peak around −0.4 V. Surprisingly, the voltammograms do not give evidence of $Fe^{II}(L)$ formation. This may be due to the high reactivity of $Fe^{II}(L)$; high speed voltammetry at ultramicroelectrodes is required to answer this question. Nevertheless, under electrolysis it appears that Fe—O bond cleavage is achieved easily through the mixed valence dinuclear compound $[(L)Fe^{III}—O—Fe^{II}(L)]^-$. Is this cleavage possible through a chemical route?

Chemical cleavage of the Fe—O *bond*

As the monomeric complexes are synthesized with an axial chloride ion,[13,16,29,30] we have studied the influence of Cl^- on the redox properties of $[Fe(L)]_2O$. To $[Fe(L)]_2O$ solutions was added equivalent quantities of Et_4NCl and the analysis carried out by recording the voltammograms.

Under stationary conditions (Fig. 7), the Cl^- addition presented two effects:

(i) At first, vs the original voltammogram with no Cl^- ions added, we observed the appearance of a new reduction wave at −0.45 V whose diffusion current increased when the Cl^- concentration increased. This reduction wave is attributed to the reduction process of $Fe^{III}(L)Cl$. This implies Fe—O bond cleavage by Cl^- ions according to:

$$[(L)Fe—O—Fe(L)] + 2Et_4NCl \rightarrow 2(L)Fe^{III}Cl + (Et_4N)_2O. \quad (8)$$

(ii) Moreover, Cl^- ions affect the shape of the reduction wave of $[Fe(L)]_2O$. The half-wave potential is highly shifted towards the anodic potential when Cl^- ions are added: the reduction becomes easier. The diffusion currents of this wave are enhanced as for a catalytic process. The ratio (I_D with Cl^-/I_D without Cl^-) goes up to 1.8 for one Cl^- equivalent per iron, then decreases because of the transformation of $[Fe(L)]_2O$ into $(L)Fe^{III}Cl$. As to the diffusion current of the first wave [reduction of $(L)Fe^{III}Cl$], it is nearly linear with the Cl^- concentration, but could not be related by least squares fittings to an equilibrium constant. Since the diffusion currents of $[Fe(L)]_2O$ and $(L)Fe^{III}Cl$ depend on the Cl^- concentration, their values cannot be used to determine the complex concentrations and then an eventual dissociation constant.

Under non-stationary conditions (Fig. 8), the voltammograms are in agreement with the ones recorded under stationary conditions. When Cl^- is added, the reduction peak of $(L)Fe^{III}Cl$ is observed and confirms the occurrence of reaction (8). As mentioned above, the peak potentials are shifted towards anodic potentials when the Cl^- concentration increases and non-quantitative determinations could be achieved: the total current $[I_{p\,red}(L)Fe^{III}Cl + I_{p\,red}[Fe(l)]_2O]$ increases with Cl^- concentration. Concerning the kinetics, Cl^- ions affect the reversibility of $[Fe(L)]_2O$ reduction: the backward peak disappears. Moreover, the oxi-

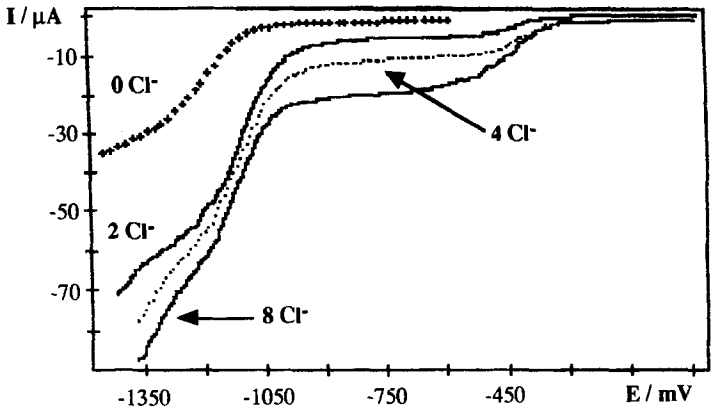

Fig. 7. Voltammograms at a rotating (1000 t min^{-1}) platinum electrode in CH_2Cl_2–Bu_4NPF_6 (0.1 mol dm^{-3}) of $[Fe(SALEN)]_2O$, 1 mmol dm^{-3} for various Et_4NCl additions.

dation peak of the hydroxy complex [around −0.6 V for SALOPH and generated by reaction (6)] disappears, while the oxidation peak of $(L)Fe^{II}Cl$ appears and increases when the Cl^- concentration increases. So Cl^- ions cleave the Fe—O bond according to reaction (8), but also interact in the reduction process of $[Fe(L)]_2O$: Cl^- ions shift the bond cleavage of the mixed valence compound to the right [reaction (8)] and substitute OH^- in the hydroxy species. From Fig. 8, one can see that the peak ratio for the (L)FeCl complex [$RI_p = I_{p\,ox}(L)Fe^{II}Cl/I_{p\,red}(L)Fe^{III}Cl$] becomes higher than 1 for high Cl^- concentrations. This resulting excess of $(L)Fe^{II}Cl$ at the electrode comes from Fe—O bond cleavage during the reduction process of $[Fe(L)]_2O$.

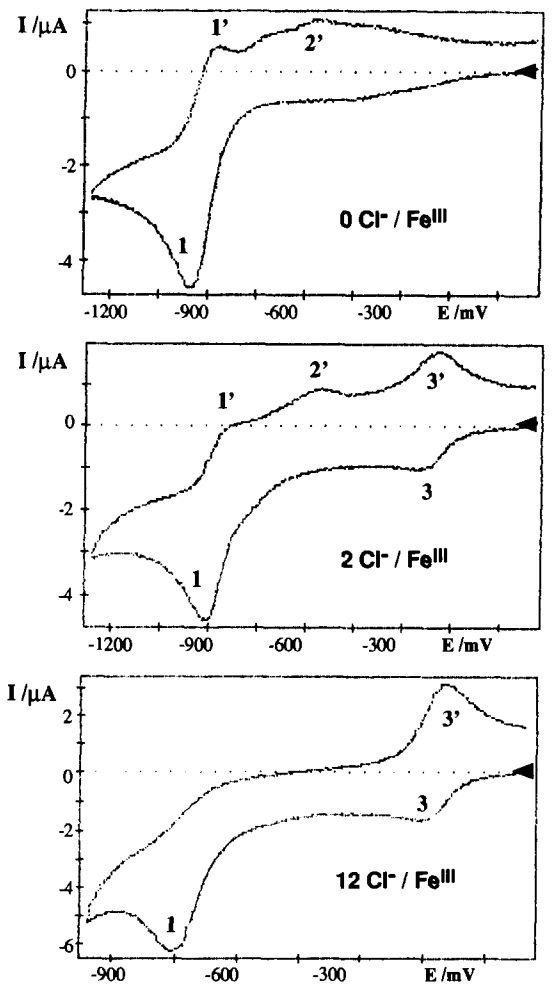

Fig. 8. Cyclic voltammograms at a platinum electrode in CH_2Cl_2–Bu_4NPF_6 (0.1 mol dm^{-3}) of $[Fe(SALOPH)]_2O$, 1 mmol dm^{-3} for various Et_4NCl additions ($v = 0.1$ V s^{-1}).

The reduction process of $[Fe(L)]_2O$ appears rather complicated. Polynuclear units were postulated in order to explain the reduction of [Fe (SALEN)]$_2$O.[11] Such species can explain the passivation phenomena observed in the study by their deposition onto the electrode surface. On the contrary, in solution it appears that the dinuclear μ-oxo $[Fe(L)]_2O$ complexes are easily cleaved into monomeric species. In order to check the formation of high nuclearity compounds, we studied the interaction of $[Fe(L)]_2O$ and $(L)Fe^{III}Cl$ (Fig. 9). In solution, the voltammogram of $(L)Fe^{III}Cl$ presents the pattern of a quasi-reversible system (9). When $[Fe(L)]_2O$ was added, we observed the two reduction processes of $(L)Fe^{III}Cl$ and $[Fe(L)]_2O$. However, the reduction peak current of $(L)Fe^{III}Cl$ increased and the reversibility of this system vanished ($RI_p = I_{p\,ox}/I_{p\,red}$ decreases) when the $[Fe(L)]_2O$ concentration increased. The pattern of the $[Fe(L)]_2O$ reduction was also modified: the electrochemical system appeared less reversible and the reduction peak current of $[Fe(L)]_2O$ was lower than expected. Moreover, the oxidation peak of the hydroxy species was enhanced. When the potential scan rate was increased, the monomer redox couple appeared reversible and the oxidation peak of the

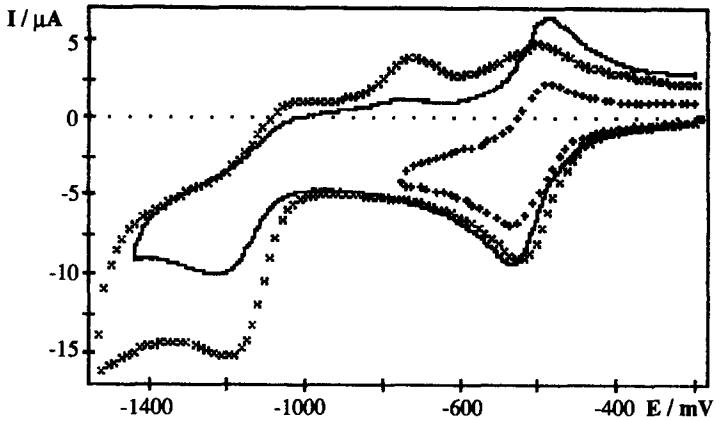

Fig. 9. Cyclic voltammograms at a platinum electrode in CH_2Cl_2–Bu_4NPF_6 (0.1 mol dm^{-3}) of (SALEN)$Fe^{III}Cl$, 1 mmol dm^{-3} for various $[Fe(SALEN)]_2O$ additions ($v = 0.1$ V s^{-1}). (+ + +) (SALEN)$Fe^{III}Cl$ alone, (——) with $[Fe(SALEN)]_2O$ (0.5 mmol dm^{-3}), (× × ×) with $[Fe(SALEN)]_2O$ (1 mmol dm^{-3}).

hydroxy species decreased. Under stationary conditions, the diffusion current of (L)$Fe^{III}Cl$ was also enhanced when $[Fe(L)]_2O$ was added. Taking into account the results, we propose an electron transfer reaction between electrogenerated Fe^{II} and $[Fe(L)]_2O$ according to:

$$(L)Fe^{III}Cl + e^- \rightleftharpoons (L)Fe^{II}Cl^- \quad (9)$$

$$(L)Fe^{III}—O—Fe^{II}(L) + (L)Fe^{II}Cl^- \rightarrow [(L)Fe^{III}—O—Fe^{II}(L)]^- + (L)Fe^{III}Cl. \quad (10)$$

The mixed valence dimer is when cleaved following reactions (4)–(6).

Cyclic voltammetry at micrometric electrodes

According to the proposed scheme [reactions (4)–(6)] for the reduction of $[Fe(L)]_2O$, cyclic voltammograms should give evidence of the oxidation peak of (L)Fe^{II}. This was not observed with millimetric electrodes because of the high reactivity of (L)Fe^{II}. By decreasing the electrode diameter, cyclic voltammograms can be recorded at higher potential scan rates in order to observe intermediates.[18,31] At a 100 μm platinum electrode (Fig. 10), cyclic voltammetry has been carried out for potential scan speeds from 10 up to 1800 V s^{-1}, the upper limit of the equipment. The voltammograms are different from the ones obtained at millimetric electrodes. The electrochemical reduction of $[Fe(L)]_2O$ appears more reversible but presents on the backward scan the oxidation peak of $[(L)Fe^{II}—OH]^-$, whatever the scan speed. Moreover, the oxidation peak of (L)Fe^{II} is never observed, which is not in agreement with the proposed scheme. Due to the high reactivity of (L)Fe^{II}, the hydrolysis by residual water of the mixed valence compound may thus be postulated according to:

$$[(L)Fe^{III}—O—Fe^{II}(L)]^- + H_2O \rightarrow [(L)Fe^{II}—OH]^- + (L)Fe^{III}—OH \quad (11)$$

but addition of water to the medium does not affect the voltammograms. Another explanation could be the reductive cleavage of $[Fe(L)]_2O$ by (L)Fe^{II} as mentioned above [reaction (10)]. By classical voltammetry, this reaction appears slow and should be blocked by high speed voltammetry. The disappearance of (L)Fe^{II} could be due to an intramolecular electron transfer from Fe^{II} to the ligand which yields a dimer, as reported for the reduction of Ni(SALOPH).[22,23] The dimer is produced by C—C bond formation through the reduction of the imine bond:

$$2[Fe^{II}(L)]^- \rightarrow 2[Fe^{III}(L^\circ)]^- \rightarrow [Fe^{III}_2(L'_2)]^{2-}. \quad (12)$$

The dimerization rate constant has been estimated to be 6×10^5 dm^3 mol^{-1} s^{-1} for Ni(SALOPH).[22] However, electrochemical studies of (L)$Fe^{III}Cl$ complexes[9] did not give evidence of such a pathway because the reduction potential of (L)$Fe^{III}Cl$ is around 1 V more anodic than the one of Ni^{II}(L) and is not able to transfer an electron towards the ligand. Nevertheless, as the reduction potential of $[Fe(L)]_2O$ is of the same order of magnitude as that of Ni(SALOPH) this intramolecular electron transfer may proceed. Such a reaction would explain the difference between chemical and electrochemical Fe—O bond cleavage. The chemical cleavage by Cl^- ions yields unambiguously (L)$Fe^{III}Cl$, while by electrochemistry only the hydroxy species

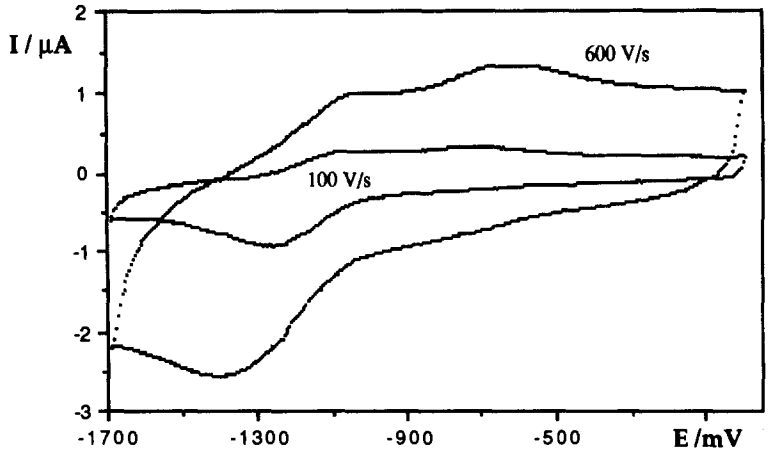

Fig. 10. Cyclic voltammograms at a platinum electrode (diam 100 μm) in CH_2Cl_2–Bu_4NPF_6 (0.1 mol dm^{-3}) of (SALEN)$Fe^{III}Cl$, 1 mmol dm^{-3}.

are observed: no oxidation peak of $(L)Fe^{II}$ or reduction peak of $(L)Fe^{III}$ is present on the voltammograms.

The electrochemical reduction of $[Fe(L)]_2O$ is rather complicated and is reduced to the proposed scheme in order to carry out simulations with Gosser's program.[32] So, we take into account reactions (3)–(6): an ECE scheme where the reaction is a fast equilibrium and disappears through the irreversible dimerization reaction (12) [the rate constant is estimated as 6×10^5 dm^3 mol^{-1} s^{-1} as for Ni (SALOPH)].[22] The standard rate electron transfer constants are also estimated through the peak potential separation ΔE_p.[26] In CH_2CL_2, for L = SALEN, we obtained the following results. As regards the first electron transfer, reaction (3), we obtained a standard rate electron transfer constant k^0 of 0.05 cm s^{-1} with $\alpha = 0.5$ and $E^0 = -1.18$ V. Taking into account chemical Fe—O bond cleavage, reaction (4), the rate constant k_4 is estimated as 100 s^{-1}. The hydroxy redox couple, reaction (6), presents a standard rate electron transfer constant k^0 of 0.2 cm s^{-1} with $\alpha = 0.5$ and $E^0 = -0.8$ V. The rate constant k_4 depends on the nature of the Schiff base and decreases when the ligand delocalization increases:

$$k_4(\text{AEAP}) = 600\ s^{-1};\ k_4(\text{SALEN}) = 100\ s^{-1};$$

$$k_4(\text{SALOPH}) = 40\ s^{-1}.$$

The rate constant k_4 is quite high and is in agreement with the cyclic voltammograms and the electrochemical behaviour under stationary conditions. In the latter case, the electrochemical reduction of $[Fe(L)]_2O$ proceeds through a global two-electron exchange.

CONCLUSION

Transition metal complexes play a very important role in many electrochemical catalytic processes.[33] Schiff base complexes have been recognized as powerful catalysts. Among these compounds, iron Schiff base complexes have been fully described as chemical models of biological systems but have received less attention for their electrochemical properties. We focussed here on the reduction of the μ-oxo dimer (L)Fe—O—Fe(L). From these results it appears that the Fe—O bond can be cleaved either chemically or electrochemically. This property is quite promising for dioxygen activation and will be the subject of a forthcoming paper. Moreover, these complexes may manage C—H activation as with similar compounds.[34]

Acknowledgement—The "Conseil Régional de la Région Midi-Pyrénées" is gratefully acknowledged for the financial support of our research.

REFERENCES

1. J. P. Collman, T. R. Halbert and K. S. Suslik, in *Metal Ion Activation of Oxygen* (Edited by T. Spiro). Wiley Interscience, New York (1980); *Molecular Mechanisms of Oxygen Activation* (Edited by O. Hayaishi). Academic Press, New York (1974).
2. L. Que Jr., *Coord. Chem. Rev.* 1983, **50**, 73; L. Que Jr. and A. E. True, *Prog. Inorg. Chem.* 1990, **38**, 97.
3. K. S. Murray, *Coord. Chem. Rev.* 1974, **12**, 1.
4. Y. Dong, S. Menage, B. A. Brennan, T. E. Elgren, H. G. Jang, L. L. Pearce and L. Que Jr., *J. Am. Chem. Soc.* 1993, **115**, 1851 and refs therein.
5. S. Menage, Y. Zang, M. P. Hendrich and L. Que Jr. *J. Am. Chem. Soc.* 1992, **114**, 7786.

6. M. S. Mashuta, R. J. Webb, J. K. McCuster, E. A. Schmitt, K. J. Oberhausen, J. F. Richardson, R. M. Buchanan and D. N. Hendrickson, *J. Am. Chem. Soc.* 1992, **114**, 3815 and refs therein.
7. R. N. Mukherjee, T. D. P. Stack and R. H. Holm, *J. Am. Chem. Soc.* 1988, **110**, 1850.
8. B. S. Snyder, G. S. Patterson, A. J. Abrahamson and R. H. Holm, *J. Am. Chem. Soc.* 1989, **111**, 5214.
9. B. Carre, J. P. Costes, J. B. Tommasino, D. de Montauzon, F. Soulet and P. L. Fabre, *Polyhedron* 1993, **12**, 641.
10. R. N. Mukherjee, A. J. Abrahamson, G. S. Patterson, T. D. P. Stack and R. H. Holm, *Inorg. Chem.* 1988, **27**, 2137.
11. S. E. Wenk and F. A. Schultz, *J. Electroanal. Chem.* 1979, **101**, 89.
12. J.-P. Costes, G. Gros, M.-H. Darbieu and J.-P. Laurent, *Inorg. Chim. Acta* 1982, **60**, 111.
13. P. Pfeiffer, E. Breith, E. Lübbe and T. Tsumaki, *Justus Liebigs Ann. Chem.* 1993, **503**, 84.
14. J. Lewis, F. E. Mabbs and A. Richards, *J. Chem. Soc. (A)* 1967, 1014.
15. F. Corazza, C. Floriani and M. Zehnder, *J. Chem. Soc., Dalton Trans.* 1987, 709.
16. N. Masumoto, K. Kimoto, K. Nishida, A. Ohyoshi and Y. Maeda, *Chem. Lett.* 1984, 479.
17. P. Cassoux, R. Dartiguepeyron, P. L. Fabre and D. de Montauzon, *Actual. Chim.* 1985, **1–2**, 79; *Electrochim. Acta* 1985, **30**, 1485.
18. J.-B. Tommasino, Thèse no. 1328 de l'Université Paul Sabatier, Toulouse (1992).
19. P. Audebert, P. Capdevielle and M. Maumy, *New J. Chem.* 1991, **15**, 235; C. P. Horwitz and R. W. Murray, *Molec. Cryst. Liq. Cryst.* 1988, **160**, 389; J. K. Blaho, K. A. Goldsby and L. A. Hoferkamp, *Polyhedron* 1988, **8**, 113; F. Bedioui, E. Labbe, S. Gutierrez-Granados and J. Devynck *J. Electroanal. Chem.* 1991, **301**, 267.
20. P. Audebert, P. Hapiot, P. Capdevielle and M. Maumy, *J. Electroanal. Chem.* 1992, **338**, 269.
21. J. R. Dorfman, J. J. Girerd, E. D. Simhon, R. T. D. P. Stack and R. H. Holm, *Inorg. Chem.* 1984, **23**, 4407.
22. A. A. Isse, A. Gennaro and E. Vianello, *Electrochim. Acta* 1992, **37**, 113.
23. S. Gambarotto, F. Urso, C. Floriani, A. Chiesi-Villa and C. Guastini, *Inorg. Chem.* 1983, **22**, 3966.
24. S. Gambarotta, C. Floriani, A. Chiesi-Villa and C. Guastini, *J. Chem. Soc., Chem. Commun.* 1982, 756; S. Gambarotta, M. Mazzati, C. Floriani and M. Zehnder, *J. Chem. Soc., Chem. Commun.* 1984, 116.
25. F. Lloret, J. Moratal and J. Faus, *J. Chem. Soc., Dalton Trans.* 1983, 1743, 1749.
26. R. S. Nicholson and I. Shain, *Anal. Chem.* 1964, **36**, 706.
27. F. Lloret, J. Moratal and J. Faus, *J. Chem. Soc., Dalton Trans.* 1983, 1749.
28. F. Lloret, M. Mollar, J. Faus, M. Julve, I. Castro and W. Diaz, *Inorg. Chim. Acta* 1991, **189**, 195.
29. B. W. Fizsimmons, A. W. Smith, L. F. Larkworthy and K. A. Rogers, *J. Chem. Soc., Dalton Trans.* 1973, 676.
30. N. Matsumoto, K. Kimoto, A. Ohyoshi and Y. Maeda, *Bull. Chem. Soc. Jpn* 1984, **57**, 3307.
31. M. Fleischman, S. Pons, D. R. Rolison and P. P. Schmidt, in *Ultramicroelectrodes*. Datatech Systems Inc, Morgaton (1987).
32. D. K. Gosser and P. H. Reiger, *Anal. Chem.* 1988, **37**, 115.
33. O. N. Efinov and V. V. Strelets, *Coord. Chem. Rev.* 1990, **99**, 15.
34. S. Menage, J. M. Vincent, C. Lambeaux, G. Chottard, A. Grand and M. Fontecave, *Inorg. Chem.* 1993, **32**, 4766; R. A. Leising, J. H. Kim, M. A. Perez and L. Que Jr., *J. Am. Chem. Soc.* 1993, **115**, 9524.